MARINE BOUNDARY-LAYER VARIABILITY OVER THE INDIAN OCEAN DURING INDOEX (1998)

VIJAYAKUMAR MANGHNANI[1], SETHU RAMAN[1]*, DEVDUTTA S. NIYOGI[1], VINAYAKA PARAMESWARA[1], JOHN M. MORRISON[1], S. V. RAMANA[2] and J. V. S. S. RAJU[3]

[1]*Department of Marine, Earth and Atmospheric Sciences, Box 8208, NCSU, Raleigh, NC 27695, U.S.A.;* [2]*Space Physics Laboratory, Vikram Sarabhai Space Center, Trivandrum, India;* [3]*Center for Atmospheric and Ocean Sciences, Indian Institute of Sciences, Bangalore, India*

(Received in final form 15 May 2000)

Abstract. The variability in boundary-layer structure over the Indian Ocean during a north-east monsoon and the factors influencing it are investigated. This study was made possible as a component of the Indian Ocean Experiment (INDOEX), conducted from February 19 to March 30, 1998. The data used are, surface-layer mean and turbulence measurements of temperature, humidity and wind, and vertical soundings of temperature and humidity. Significant spatio-temporal variability was observed in the boundary-layer structure throughout the cruise. The ITCZ was characterized as the region with strongest winds and maximum surface turbulent fluxes of momentum and heat. One of the important findings from this study was a strong influence of continental air masses on the boundary-layer structure in the Northern Hemisphere, even at a distance of 600 km off the Indian coast. This was generally evident in the form of an elevated plume of dry continental air between altitudes of 1500 m and 2700 m. Advection of continental aerosols in this layer presents potential for significant entrainment into shallow clouds in this region, which eventually feed deeper clouds at the ITCZ. This finding provides an explanation for anomalous higher aerosol concentrations found during previous studies. The structure of the marine boundary layer was influenced by various factors such as proximity to land, an anomalous warm pool in the ocean and the ITCZ. In the southern hemisphere, the boundary-layer height was primarily governed by surface-layer sensible heat flux and was found to be highest in the vicinity of the ITCZ. North of the equator it was strongly influenced by land-air-sea interactions. In addition to this synoptic modulation, there was also a significant diurnal variability in the boundary-layer height.

Keywords: Indian Ocean, INDOEX, ITCZ, Marine boundary layer, North-east monsoon.

1. Introduction

One of the primary objectives of the Indian Ocean Experiment (INDOEX) is to understand the extent to which the continental aerosols, both natural and anthropogenic, are transported over clean ocean regions thousands of kilometres away from the sources and to characterize the meteorological processes responsible for this transport. The transport of aerosols from source regions on the continents to remote oceans could play a significant direct as well as indirect role in global radiative

* Corresponding author: E-mail: sethu_raman@ncsu.edu

Boundary-Layer Meteorology **97:** 411–430, 2000.

forcing (IPCC, 1994). In the boreal winter, the prevalent northerly winds and the presence of a significant source of pollutants to its northern boundary, make the tropical Indian Ocean an ideal natural laboratory to study the export of aerosols and their influence on climate (Ramanathan et al., 1995).

Though it is established that meteorological processes over the ocean play an important role in the spatial distribution and residence times of aerosols, these phenomena are not well understood, primarily due to lack of adequate data over the ocean. Therefore, in addition to the aerosol and radiation measurements, detailed spatial and temporal measurements to sample the boundary-layer and the air-sea fluxes were carried out during this second and final pre-INDOEX (1998). The meteorological data collected in this cruise were in the form of vertical soundings of temperature and humidity in the troposphere and measurements of surface-layer mean and turbulence parameters. The cruise on ORV Sagar Kanya was conducted from February 19 to March 30, 1998. In the first leg of the cruise (February 19–March 12), the ship traversed from Goa, India (15° N, 76° E) to Port Louis, Mauritius (15° S, 60° E) (Figure 1) with an extended halt of 3 days (February 27–March 1) off Kaashidoo, Maldives (4.9° N, 73° E). In the return leg (March 17–March 30), the ship traversed from Port Louis, Mauritius to Goa, India. Over the region of interest the synoptic conditions remain essentially the same, with a high pressure system over the Indian subcontinent and north-easterly winds over the Indian Ocean north of the ITCZ. The ITCZ itself migrated to the north during the experiment.

The objectives of this paper are to analyze the boundary-layer structure and its spatio-temporal variability over the Indian Ocean during the period of the pre-INDOEX 98. Some important questions that have been addressed are: what is the structure of the boundary layer over the Indian Ocean during the north east Monsoon period? What are the local factors that influence the spatio-temporal variability in the boundary-layer height? Can the Indian Ocean be split into regimes where certain processes play a more dominant role in influencing the boundary layer? The analysis further provides insights into the mesoscale structure of the surface heat and momentum fluxes and the influence of these fluxes on the observed boundary-layer structure.

2. Data and Methods

The mean and turbulence measurements in the atmospheric surface layer were made by setting up instruments on a retractable steel boom fitted in the bow of the ship. The height of the boom above sea-level was 10 m. The platform was designed so as to withstand high winds and was guyed to stationary supports on the deck. The relevant instruments for this study are a three-axis Gill Propeller Anemometer for turbulence, a humicap for relative humidity fluctuations, and a platinum resistance thermistor for dry bulb air temperature variations. Turbulence measurements of

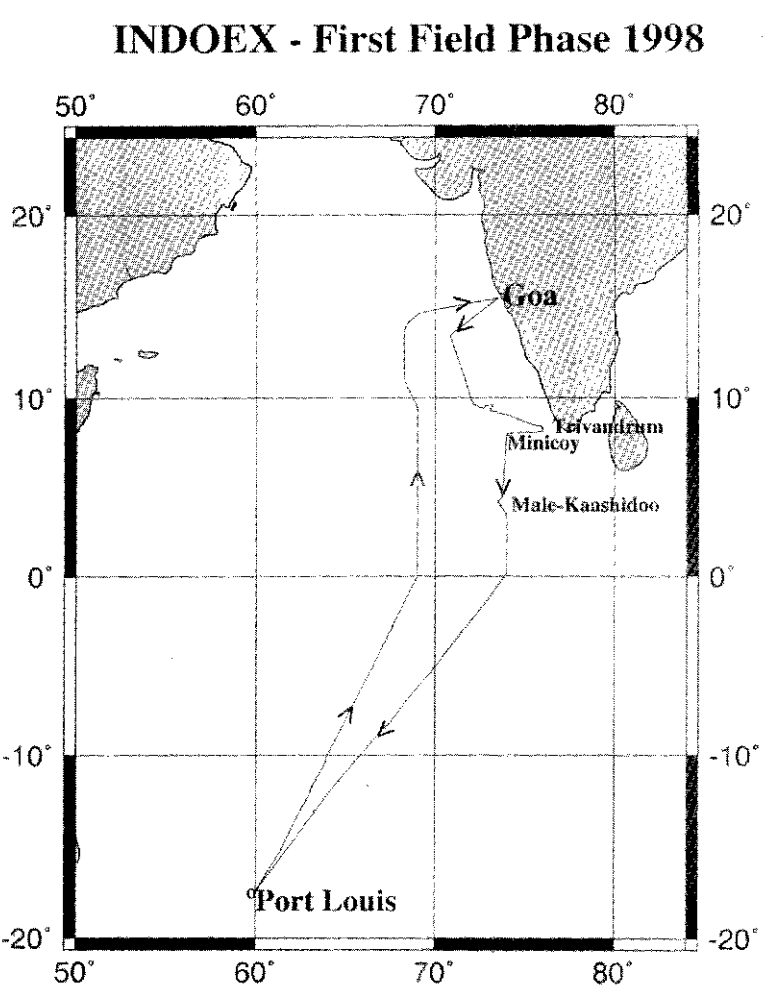

Figure 1. The cruise track and station halts during the pre-INDOEX. The cruise was from February 19 to March 30, 1998.

wind speed and temperature were made four times daily, for one hour periods at a frequency of 5 Hz, for this the ship was stopped and made stationary. On the other hand, measurements of mean values (one-minute averages) of temperature, wind speed, direction, and relative humidity, were made throughout the experiment. The wind vector was corrected for ship motion, using information collected through the ship mounted GPS.

Wind stress and the sensible heat fluxes were estimated using the Ogive-Asymptotic approach (Desjardins et al., 1989). The technique involves testing of the cospectra of a turbulent flux to inspect it for inclusion of all flux-carrying

wavelengths. Friction velocity, u_*, was calculated using the momentum flux estimated through the Ogive-Asymptotic method following the relation,

$$u_*^2 = \frac{\tau_o}{\rho}, \tag{1}$$

where τ_o is the surface wind stress, and ρ is the density of air.

The coefficient for latent heat exchange, C_h, was calculated using the derived u_* and stability parameters, following Zhang and McPhaden (1995),

$$C_h = \frac{k^2}{\left[\ln \frac{z}{z_o} - \psi_m(x)\right]\left[\ln \frac{z}{z_t} - \psi_h(x)\right]}. \tag{2}$$

For this study all the measurements were made at a height of 10 m over the sea. The roughness length, z_o, is estimated from the wind stress observations through the profile relationship. The thermal and moisture roughness constant, z_t, is set to 2×10^{-5} m, following Geernaert (1987).

The stability functions ψ_h and ψ_m for neutral and convectively unstable atmospheric conditions are those suggested by Panofsky et al. (1960), as,

$$\psi_h = 2 \ln\left(\frac{1+x^2}{2}\right), \tag{3}$$

$$\psi_m = 2 \ln\left(\frac{1+x}{2}\right) + \ln\left(\frac{1+x^2}{2}\right) - 2 \tan^{-1} x + \frac{\pi}{2}. \tag{4}$$

Here, x is a non-dimensional variable defined by

$$x = \left(1 - \gamma \frac{z}{L}\right)^{1/4}, \tag{5}$$

where z/L is the stability parameter of the surface air, L is the Obhukov length estimated using momentum and sensible heat fluxes. γ is a constant determined empirically. A value of 16 is used in this study following Paulson (1970). In the free convection limit ($z/L \ll -1$), the stability functions are slightly different from those above (the KEYPS representation). But since there is significant overlap in their effect over a large range of z/L, following Paulson (1970) and Liu et al. (1979), one can apply these equations to free convection conditions as well. For stable atmospheric conditions, a simpler form suggested by Large and Pond (1982) is used

$$\psi_h = \psi_m = -7 \frac{z}{L}. \tag{6}$$

A total of 47 vertical CLASS (Cross Chain Loran Atmospheric Sounding System) sondes were launched during the cruise. These soundings provided vertical

profiles of pressure, temperature and humidity in the troposphere. The soundings were taken daily at 0800 and 1500 LT (and at 2100 LT on some days) to capture the diurnal evolution of the boundary layer. The boundary-layer height was estimated from virtual potential temperature (θ_v) and equivalent potential temperature (θ_e) profiles. The accuracy of the boundary-layer heights so estimated can be adjudged within 50 m. The entrainment zone is estimated by using the profiles of both θ_v and humidity, and by detecting the point at which the slope of the inversion layer changes. The values of the θ_v in the mixed layer and the difference in θ_v across the entrainment zone were estimated from individual profiles. The rate of change of θ_v with height, $(\partial\theta_v/\partial z)$, across the entrainment zone was used as a measure to quantify the capping inversion over the mixed layer.

The concentrations of aerosols in the lower atmosphere are directly influenced by the strength of the vertical mixing in the boundary layer and the extent to which free-atmospheric air is entrained into the boundary layer. The convective potential of the boundary layer is best estimated using the convective velocity scale (w_*), estimated as,

$$w_* = \left[\frac{g z_i}{\theta_v}\overline{w'\theta'}\right]^{1/3}, \tag{7}$$

where z_i is the boundary-layer height, $w'\theta'$ is the sensible heat flux, $g = 9.8$ m s^{-2} is the acceleration due to gravity.

The entrainment velocity is an important parameter in estimating the rate of change of aerosol concentration in the boundary layer. Since it is not practical to directly measure w_e, a variety of indirect methods and parametrization have been developed (Stull, 1976; Deadroff, 1979) to arrive at first-order estimates of w_e. When interpreted in light of the basic assumptions made during the parametrization, these results may provide insight into the entrainment characteristics of the boundary layer. In this study the entrainment velocity for a cloud-free mixed layer, has been estimated following Stull (1988) as,

$$w_e = 2\frac{C_1 w_*^3 + C_2 u_*^3}{d_1 \Delta\theta_v g/\theta_v}, \tag{8}$$

where the constants are $C_1 = 0.0167$ and $C_2 = 0.5$, $\Delta\theta_v$ is the change in virtual potential temperature across the entrainment zone, d_1 is the distance between the top of the mixed layer and the height where the heat flux profile crosses zero and has been estimated as,

$$d_1 = z_i \frac{\nabla\theta_v w_e}{\overline{w'\theta'} + \nabla\theta_v w_e}. \tag{9}$$

The first term in the numerator in (8) accounts for the effect of buoyant production, while the second term accounts for mechanical production at the surface. Mechanical production at the top of the mixed layer (due to wind shear) has been neglected, leading to an under estimation of w_e.

The locations of the ITCZ during the experiment were identified through an analysis of satellite cloud images. The ITCZ was around 9° S in the first leg of the experiment (19 February to 12 March) and at 5° S during the return leg of the cruise (17 March to 30 March). In addition to the atmospheric data, the sea surface temperature (SST) and mixed-layer depth of the ocean were also measured at all stations. SST was measured using a bucket thermometer; the error associated with the measured SST is of the order of 0.5K. The mixed-layer depth of the ocean was estimated studying the data acquired from SeaBird CTD profiles.

3. Results

3.1. Mean state

Figures 2a–d show the hourly mean values of wind speed, wind direction, air temperature and specific humidity for the entire cruise. In order to depict the diurnal variability as well as the spatial trends in the data, they have been plotted with respect to time but the x-axis has been labeled by latitude. Along the x-axis the latitude decreases initially from 13° N to 16° S (first leg of the cruise), and then increases from 16° S to 13° N (the return leg). There was an extended halt for 3 days in the first leg (off Kaashidoo Islands, 5° N). Representation of the latitude in the x-axis along the ship track enables interpretation of the spatial as well as the temporal variability in the data. As seen in Figure 2a, in the first leg (13° N to 16° S), the wind speed decreased with the distance away from land reaching a minimum value of about 2 m s^{-1}; however, south of 5°N wind speed increased steadily until it reached a maximum value of about 10 m s^{-1} near the ITCZ (~ 9° S). During the return leg (15 March–30 March), the mean wind speed was significantly less (~3 m s^{-1}). Maximum wind speed values of about 5 m s^{-1} were observed around 5° S, which coincided with the location of the ITCZ during that period. While we did notice an increase in the wind speed towards the ITCZ it was not as strong as in the first leg. This could be attributed to the weakening of the north-east monsoon and the ITCZ during that period. Variation of wind direction for the entire cruise is shown in Figure 2b. Values of 0 and 180 represent northerly and southerly winds respectively and 90 and −90 represent easterly and westerly winds. We notice that, in the first leg the wind direction close to the Indian subcontinent was mostly north-westerly up to 5° N. At 5° N however, there was considerable variability in the observed wind direction. This variability is a result of diurnal land-sea breeze variability associated with the Kaashidoo Islands. Away from this land influence, a gradual transition of the wind direction from north-easterly to north-westerly was observed just around the observed ITCZ (9° S) following which the wind direction gradually changed to south-easterly (around 13° S). In the return leg (15 March to 30 March), as the ship progressed from south of the ITCZ towards the Indian subcontinent, the wind direction changed from south-easterly to north-easterly in the region from 5° S to 2° S.

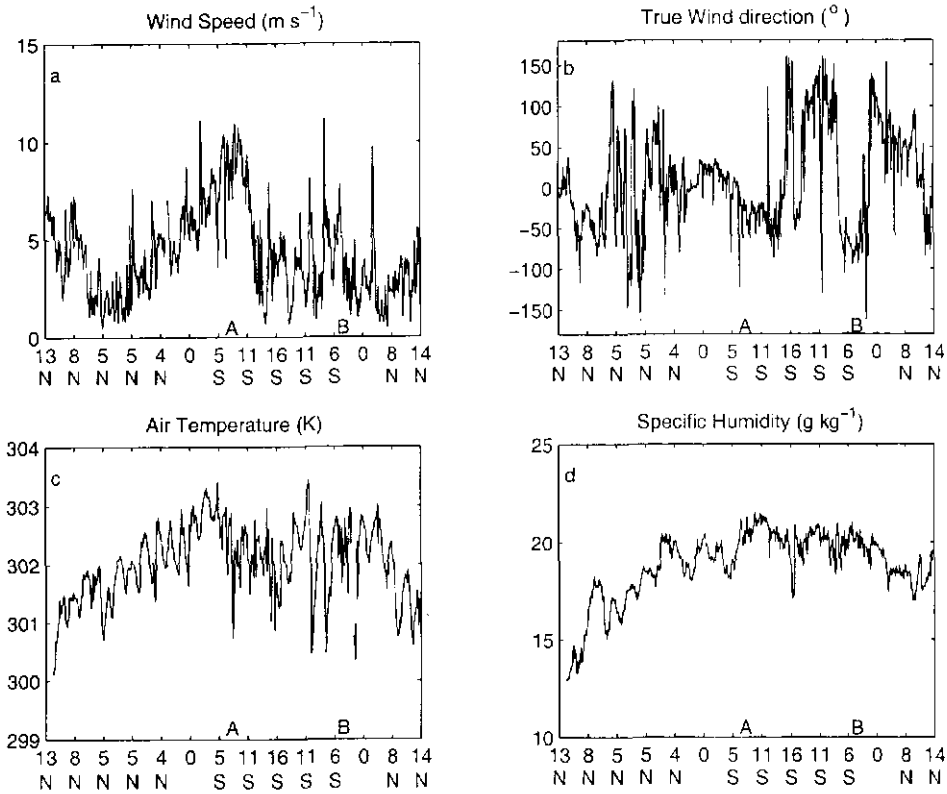

Figure 2. Mean fields of wind speed (m s^{-1}), wind direction (deg.), air temperature (K) and specific humidity (g kg^{-1}). The data are hourly and are plotted with respect to time. The x-axis is labeled by latitude. 'A' denotes the location of the ITCZ (9° S) during the first leg of the cruise. 'B' denotes the location (5° S) during the return leg.

During both legs of the experiment the surface air temperature (Figure 2c) increased as the distance from land (Indian subcontinent) increased. The air temperatures are higher than 300 K during the entire cruise. Maximum air temperature values of around 303 K were observed close to 4° S, in the first leg of the cruise. Typical diurnal variability of the order of 1 K was noted in the temperature values during the entire cruise, with warmer air temperature during the day. Highest daily temperature values were usually observed around 1700 LT and the lowest around 0600 LT. Specific humidity (Figure 2d) showed a consistent latitudinal variability with air temperature, as expected there was a general increase in the values of humidity away from land and towards the ITCZ. During the first leg of the cruise, maximum values of around 21 g kg^{-1} (80% saturated) were observed at the ITCZ (9° S). In the return leg, the latitudinal gradient of the specific humidity was not as strong as in the first leg. The specific humidity was greater than 18 g kg^{-1} (70% saturated) for most of the return leg of the cruise.

The Indian Ocean SST was typically high (> 302 K) for most of the cruise. The SST was generally low close to the Indian coast due to coastal upwelling. Warm pools of sea water (SST > 303 K) were observed near the equator during both the legs of the cruise. These warm pools were found to extend from 6°S to the equator and from 2° N to 4° N.

3.2. SURFACE-LAYER TURBULENT FLUXES

The exchange coefficients C_d and C_h (Figure 3) were used to estimate the efficiency of heat, moisture and momentum exchange between the ocean and the atmosphere above it. C_d is derived directly from the estimated momentum flux and C_h is derived using (2). These exchange coefficients are known to depend on the wind speed and surface-layer stability. In order to demonstrate the validity of the derived exchange coefficients the dependence of C_d and C_h on U is shown in Figure 3. At high wind speeds (3 m s^{-1} to 9 m s^{-1}), there was little scatter in the values of C_d and C_h. The average value of C_d was approximately 1.2×10^{-3}, while C_h increases slightly, from about 1.1×10^{-3} to 1.15×10^{-3}. However, for weak wind speeds (< 3 m s^{-1}), the values of C_d and C_h become more scattered, suggesting that the dependence of the exchange coefficient on surface-layer stability becomes more significant. We note that free convection conditions occur at low wind speeds. While, the values of C_h increase dramatically with decreasing wind speed for unstable boundary layers, there was scatter in both directions in the values of C_d. It can be further noted that the few observations of C_d and C_h at low wind speed are under stable conditions (Liu et al., 1979). In previous studies, Zhang and McPhaden (1995) and Kang et al. (1992) derived the exchange coefficients, with similar bulk formulas. Their values are close to the exchange coefficients estimated here. At higher wind speeds, the surface layer was observed to become more stable. The values of the turbulent exchange coefficients and their characteristics agree well with those observed in previous studies of the surface layer over the ocean (Liu et al., 1979; Geernaert, 1987; Smith, 1988; Bradley et al., 1991).

Wind stress and sensible and latent heat fluxes for the entire cruise are shown in Figure 4. The plots depict the latitudinal variability of the fluxes. In order to represent the general along-track latitudinal trends, low-order polynomial fits to the values in respective cruises are overlaid on the plots. The magnitudes of the fluxes are in general larger in the first leg of the cruise. In both legs of the cruise, the maximum fluxes were observed at the ITCZ locations (9° S and 5° S respectively). In the first leg (19 February to 12 March), maximum wind stress was 0.1 N m^{-2} and maximum values of latent and sensible heat fluxes were 250 W m^{-2} and 40 W m^{-2} respectively. In the return leg (15 to 30 March), the maximum values of wind stress, latent heat flux and sensible heat flux were around 0.04 N m^{-2}, 180 W m^{-2} and 15 W m^{-2} respectively. The fluxes tended to increase from 4° N until the ITCZ and then decrease to the south of the ITCZ. Close to the Indian subcontinent the distribution of the surface fluxes is more complex. The associated variability

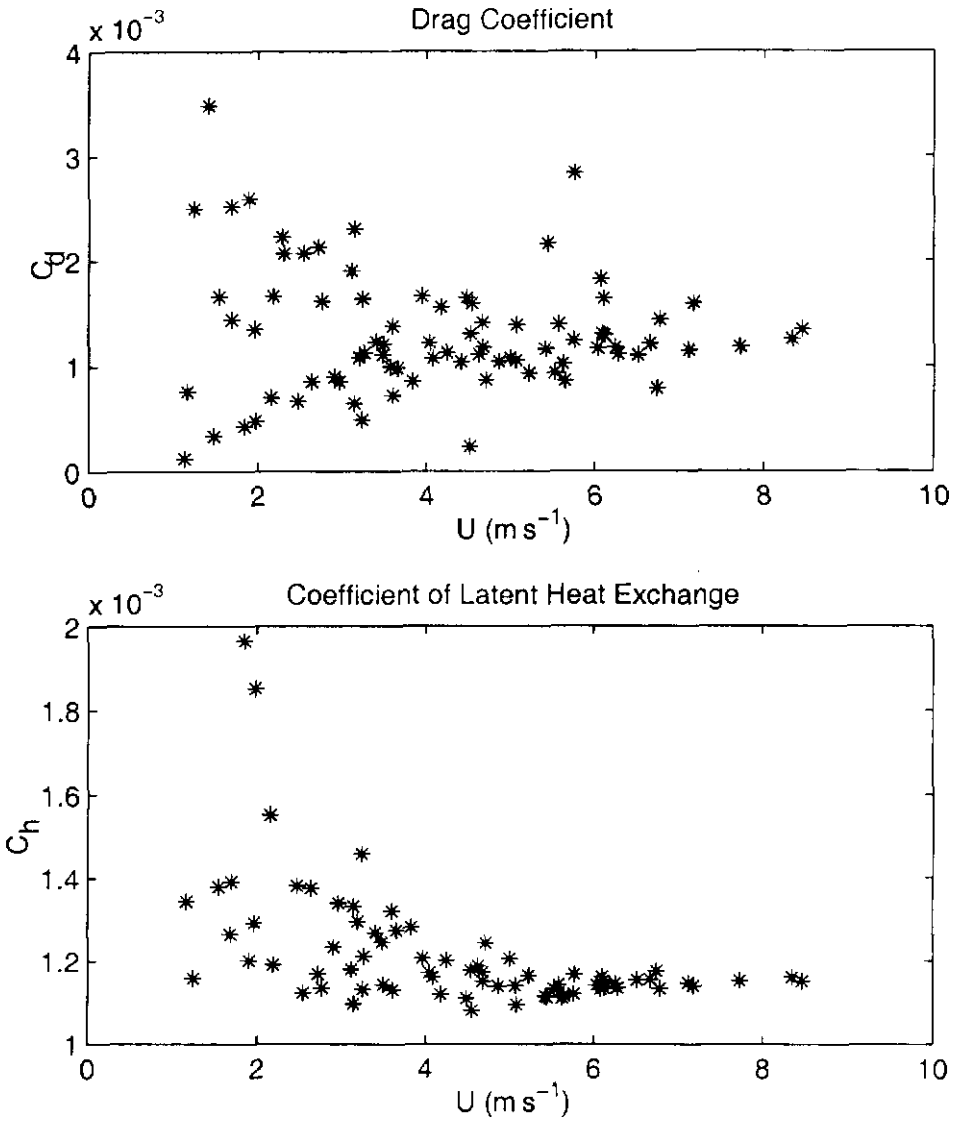

Figure 3. The variability of the drag coefficient (C_d) and the coefficient of latent heat exchange (C_h) with respect to wind speed (U m s^{-1}).

cannot be explained by the wind speed distribution (Figure 2a) alone. This suggests the possible role of surface-layer stability as influenced by coastal circulations and their diurnal variations. The range of observed fluxes during the extended stay of three days at Kaashidoo (4.9° N), in the first leg of the cruise, is represented by a vertical bar in Figure 4. As expected, due to the land-sea breezes a considerable range of temporal variability was observed at this location.

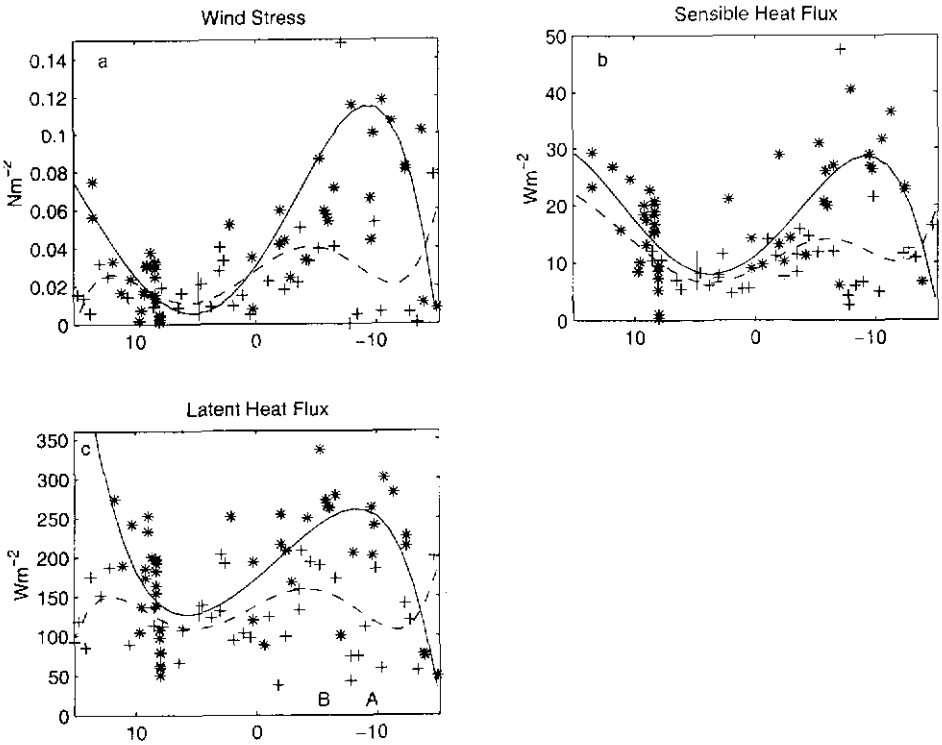

Figure 4. Latitudinal variability of wind stress (N m^{-2}), sensible heat flux (W m^{-2}) and latent heat flux (W m^{-2}). '*'s denote data from the first leg of the cruise, a polynomial fit to these data is represented by the solid line. '+'s denote data from the return leg of the cruise, the polynomial fit to these data are represented by the dashed line. The locations of the ITCZ during the forward and return legs of the cruise are denoted in (4c) by A (9° S) and B (5° S) respectively.

3.3. Boundary-Layer Height Variability

Figure 5 shows the estimated boundary-layer heights using derived profiles of θ_v and θ_e for the entire cruise. In the first leg of the cruise (February 19–March 12) the PBL heights were around 500 m close to land and higher boundary layers, around 800 m, were observed in the region from 5° S–9° S (Figure 5). This was also the region where significant increase in surface fluxes and wind speeds towards the ITCZ (9° S) were observed, as previously noted. South of the ITCZ the boundary-layer heights decreased quickly. This could be attributed to the heavy cloud cover (> 6 Oktas) over the region during that period. In the return leg of the cruise (March 17–March 30), the maxima in boundary-layer height were around 550 m and 700 m in the regions between 1° N–6° S and 4° N–10° N respectively. In the southern hemisphere, away from land, it can be hypothesized that the boundary layer is primarily influenced by the air-sea fluxes and the ITCZ dynamics; thus the lower boundary layers possibly indicate that either the ITCZ was not as intense

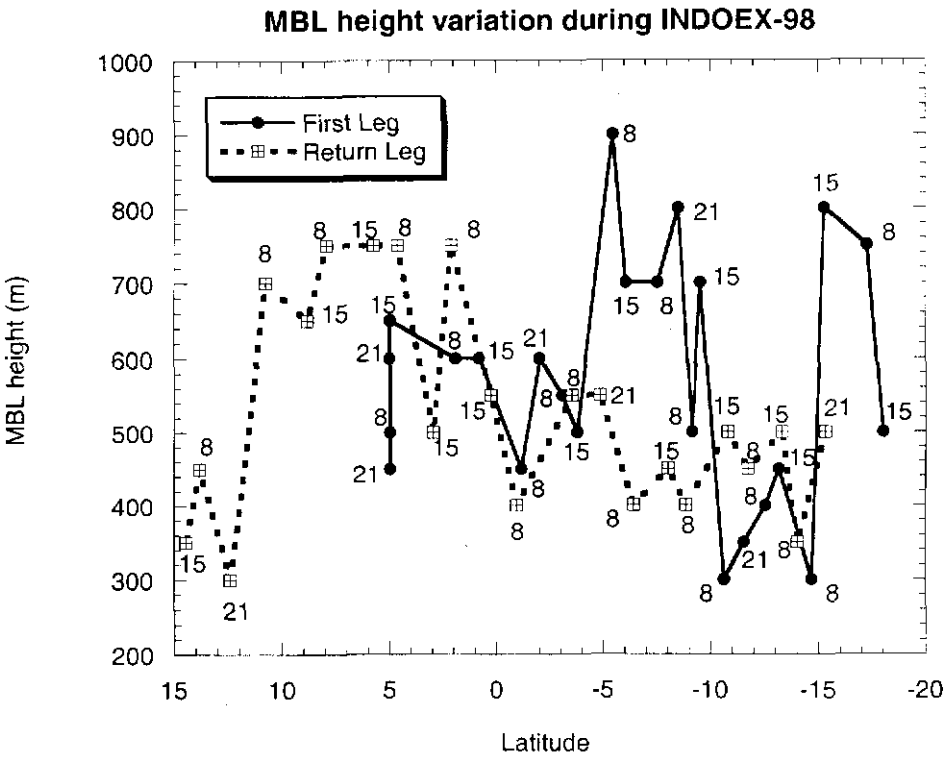

Figure 5. Latitudinal variability of boundary-layer height. The local time of each sounding launch is presented along side the data points.

or not as well established as during the first leg. In the northern hemisphere, the dry continental air mass transported by the NE monsoon winds appear to play an important role. The higher boundary-layer heights (around 3° N to 10° N) followed by very low boundary-layer heights closer to land (10° N to 13° N) during the return leg can be attributed to the complex nature of the land-sea breeze interactions with the offshore flow.

The large-scale boundary-layer characteristics over the Indian Ocean may vary depending on the influence of land-sea interactions, the ITCZ, and the presence of anomalous oceanic features (Mohanty et al., 2000). In order to understand the boundary-layer variability under these different regimes, representative profiles of the specific humidity in the lower atmosphere, close to land, near the ITCZ and over the warm pool of the ocean are plotted (Figure 6). A close look at the typical structure of the boundary layer (Figures 6 and 7) shows the influence of various phenomena on the lower atmosphere. Near the Indian subcontinent (north of 3° N) the mixed layer is topped by a strong capping inversion (Figures 6a and 7), which separates the boundary layer from the dry continental air-mass. The boundary-layer heights close to land are typically low (around 400 m). Above the boundary

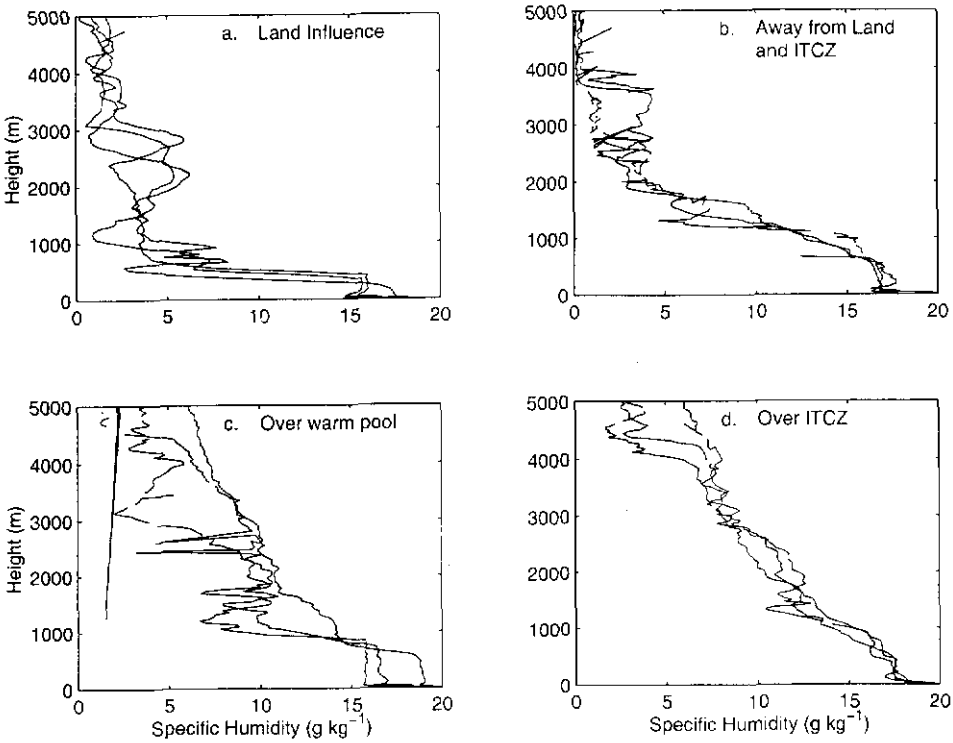

Figure 6. The spatial variability in the structure of the boundary layer, depicted through the specific humidity profiles.

layer, there is evidence of multiple layers with completely different characteristics (Figure 6a). These air masses originate from land as prevailing north-easterly winds or the land-sea breeze. They act as plumes that export aerosols into the open ocean. Figure 8 provides the profiles of virtual potential temperature and specific humidity at one such station (8° N, 69° E). This profile reveals the presence of a well-mixed dry continental air mass immediately above the boundary layer. This layer extended from about 1500 m to 270 m. This thick plume of air extended to an offshore distance of about 600 km from the land mass (Indian subcontinent). Indeed, this distance is greater than that can be explained by the conventional land-sea breeze mechanism. Krishnamurti et al. (1998), through their modeling studies suggest that the thickness of such a plume may be controlled by the diurnal variability in the boundary layer and the height of the trade inversion layer. Additionally, Mohanty et al. (2000) and Roswintiarti et al. (2000) link this plume to the presence of the Western Ghats along the coast of India.

Immediately to the south of this region (Figure 6b), the environment is neither significantly influenced by land effects nor the ITCZ dynamics. The mean boundary-layer heights are around 500 m. We also note the absence of multiple

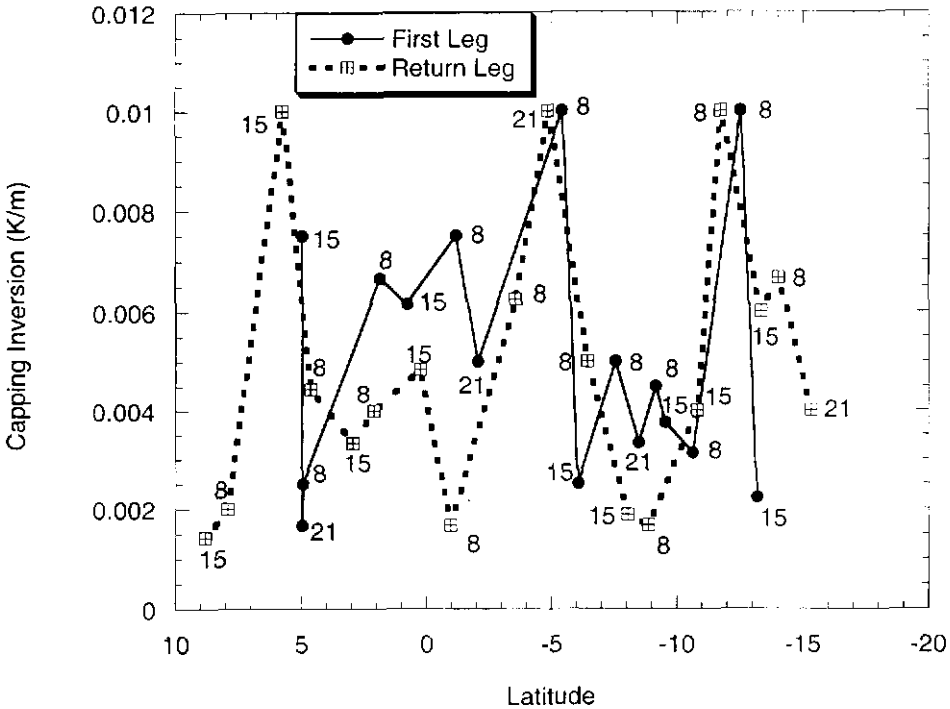

Figure 7. Variability in the capping inversion at the top of the boundary layer. The values depict the rate of change of potential temperature in the entrainment zone. The time of the sounding launch is presented along side each data point.

mixed layers above the boundary layer. The capping inversion at the top of the boundary layer is weaker in this region (Figure 7). The warm pool of ocean water (2° S–6° S) was found to be another regime that influenced the characteristics of the boundary-layer air (Figure 6c). Note that the mixed layer was not only thicker in this area (~ 600 m), but it was also capped by a strong inversion (Figure 7). As expected, the capping inversion was the weakest (Figures 6d and 7) near the ITCZ. This could be attributed to the enhanced convective activity in this zone. In the first leg of the cruise, the inversion layer on the top of the mixed layer was the weakest around 9° S (Figure 7), that is, around the ITCZ. During the return leg of the cruise the ITCZ (5° S) coincides with the location of a warm pool of water, which could have led to a well-mixed and warmer boundary layer and consequently a stronger capping inversion in that region. In summary, for the NE Monsoon over the Indian Ocean we suggest three regimes of different boundary-layer structure starting from the coast to the ITCZ.

In the southern hemisphere (Figure 5) we notice pronounced diurnal variability in the boundary-layer height. In clear sky conditions and in the absence of other large scale phenomena, the boundary layer in the afternoon was thicker by about 100 m than in the morning. The diurnal trend is clearly apparent in the return leg of

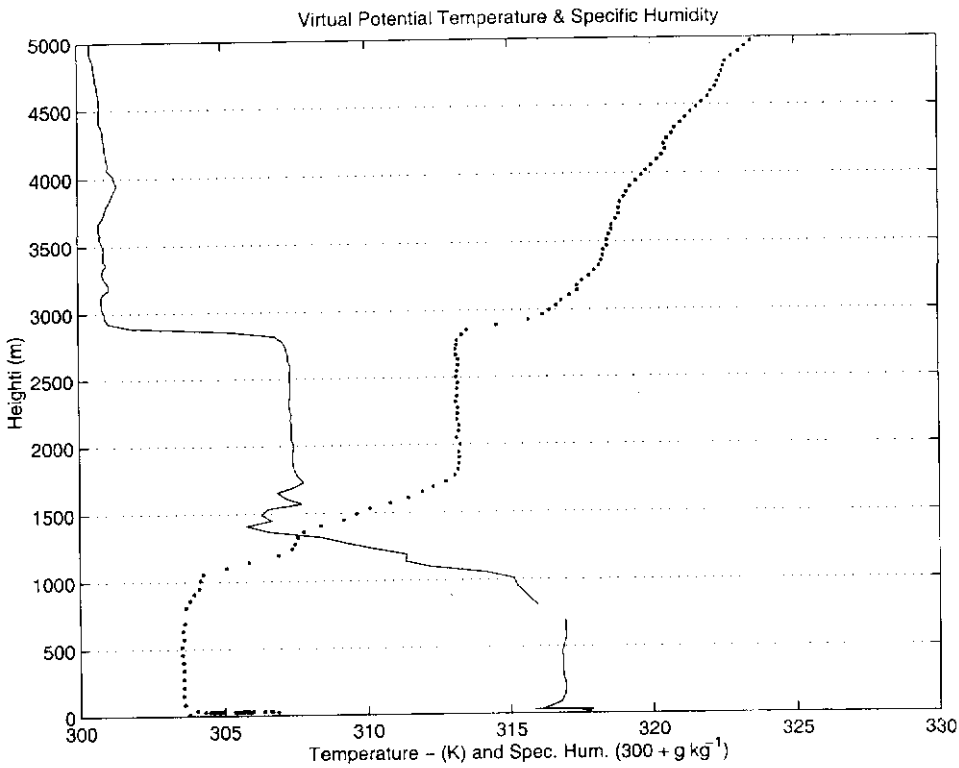

Figure 8. Vertical profile of virtual potential temperature (dotted line) and specific humidity (solid line) at (7.9° N, 69° E) approximately 600 km offshore from the Indian subcontinent. The specific humidity values have been biased by a value of 300.

the cruise when the conditions were mostly cloud free and relatively calm. In the first leg of the cruise the diurnal variability was more discernible to the south of 7.5° S until 13° S. The lack of a coherent diurnal signal in the northern hemisphere could be attributed to the strong influence of the air mass from land related to the land-sea breeze mechanism, which might serve to moderate the diurnal signal. A closer look at the θ_v profiles (not shown) reveals a dual mixed layer in the afternoon boundary layer, thus indicating enhanced mixing as the day progresses. The diurnal variability in the boundary layer is also evident in the capping inversion at the top of the boundary layer (Figure 7). The extent of the capping inversion is estimated as the rate of change in θ_v across the entrainment zone, as previously described. We note that in most cases the capping inversion is stronger in the early morning (0800 LT) boundary layer than in the afternoon (1500 LT). This is consistent with the fact that the mixing processes in the boundary layer are stronger during the later part of the day.

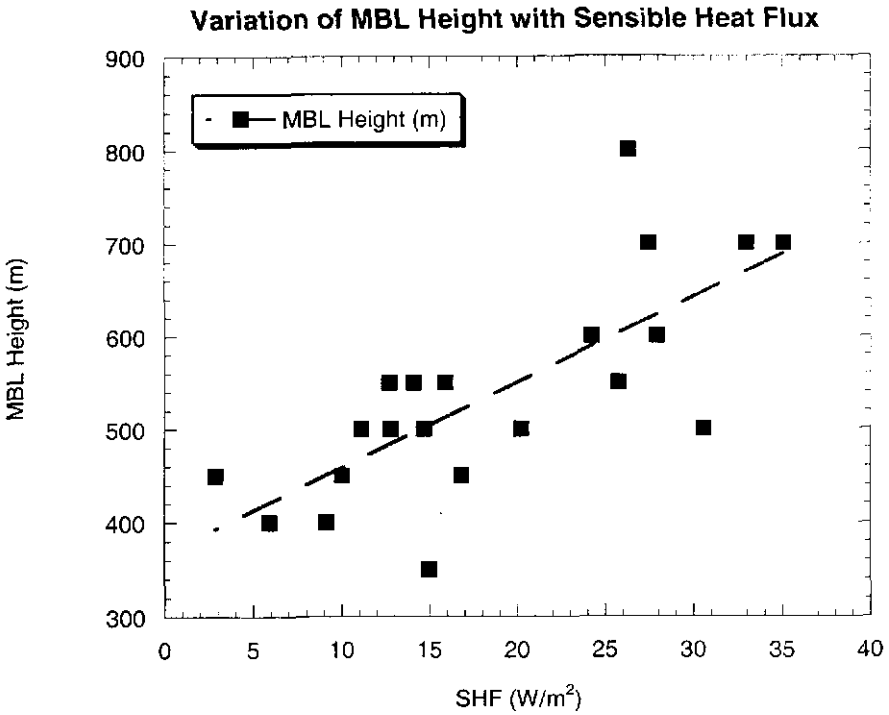

Figure 9. The variation of the marine boundary-layer (MBL) height with respect to surface sensible heat flux. Data south of 2° N have been used in this plot. Data north of 2° N were found to be more strongly influenced by processes associated with land-ocean interactions.

3.4. AIR–SEA FLUXES AND BOUNDARY-LAYER HEIGHT

Surface fluxes normally play a dominant role in the growth of the boundary layer. The height of the boundary layer is generally determined by the strength of the wind stress and the sensible heat flux over the ocean surface. Moreover, in regions close to land, the presence of dry continental air-masses at higher altitudes (brought in by the land-sea breeze mechanism) may also influence the mixing processes and growth of the boundary layer. In order to assess the relative importance of the surface fluxes on the lower atmosphere, the boundary-layer height has been plotted with respect to the sensible heat flux (Figure 9). Eliminating data that could have been influenced by the presence of a land plume (north of 2° N), we find that the boundary-layer height was approximately linearly related to the sensible heat flux at the ocean surface (Figure 9). It is observed that higher boundary layers were associated with larger sensible heat flux. This indicates that in the open ocean the boundary layer was being directly influenced by local fluxes. Observations north of 2° N (not shown), however, do not show a direct dependence of the boundary-layer height on surface fluxes, thus indicating the influence of the continental air-mass in modulating the PBL height.

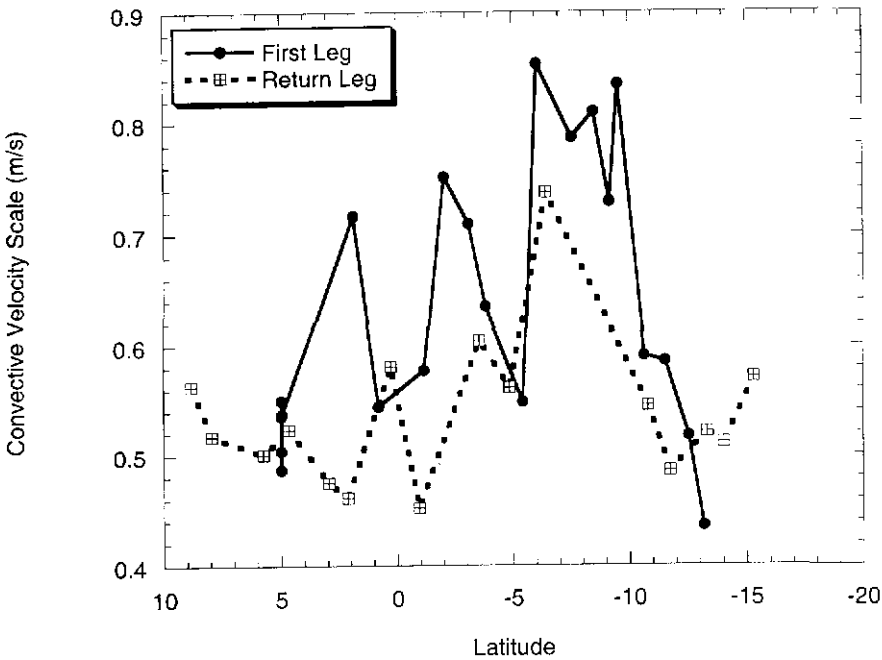

Figure 10. Latitudinal variability of the convective velocity scale.

3.5. Convective velocity scale and entrainment velocity

The convective velocity scale, w_*, (Figure 10) is an estimate of the strength of vertical motion and the convective potential in the boundary layer. Consistent with other observations, in both legs of the cruise, the convective velocity scale was maximum at the respective ITCZ locations. This indicates that there was stronger convective mixing in the boundary layer near the ITCZ. The maximum value of w_* was around 0.9 m s^{-1}. Typically, the magnitude of w_* was greater in the first leg of the cruise than in the return leg. However, in the return leg of the cruise, a steady increase in the convective velocity scale was observed to the north of equator, closer to land.

The entrainment velocity w_e (Figure 11) computed from Equation (8), quantifies the flux at the top of the mixed layer. We note considerable variability in w_e throughout the Indian ocean in both legs of the cruise. The values of w_e ranged from 0.003 to 0.009 m s^{-1}. It is noted that entrainment velocity is strongest in the southern hemisphere from 0° to 10° S, and the lower values are found from 0° to 5° N and to the south of 10° S. Observations during cloud-free conditions were used to make the estimates of w_e. We expect that these values fairly represent the entrainment characteristics over the Indian Ocean during typically clear sky conditions observed during the north-east monsoon period. However, it must be noted that close to the continent, the structure of the lower troposphere indicated

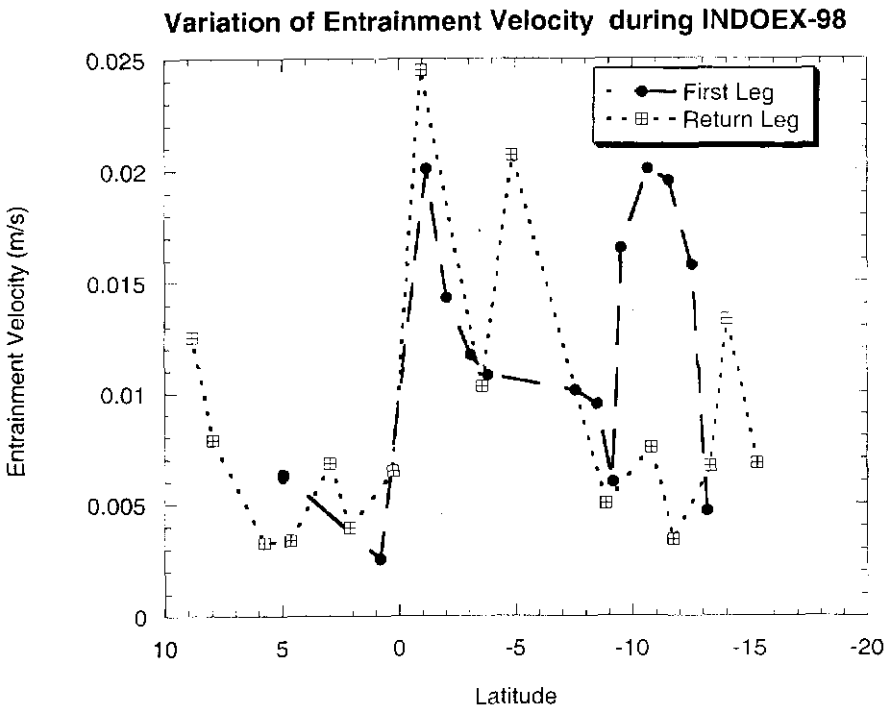

Figure 11. Latitudinal variability of the entrainment velocity.

by temperature and humidity profiles (Figure 8) reveals the existence of a thick land air mass above the boundary layer. This aerosol layer, about 1200 m thick, was found to extend as far as 600 km offshore, where shallow convective clouds generally exist. The entrainment of this aerosol rich air mass into these clouds, which in turn feed deeper ITCZ clouds, is primarily forced by horizontal advection and can be an order of magnitude larger than the convective vertical entrainment velocities. These observations explain the anomalously high aerosol and trace gas concentrations over Indian Ocean during the pre-INDOEX.

4. Summary and Conclusions

The final preliminary component of the INDOEX was conducted during the north-east monsoon (February 19–March 30, 1998). The ITCZ was characterized by peaks in momentum flux and sensible and latent heat fluxes and with thicker boundary layers in both legs of the cruise. The ITCZ was located around 9° S during the first leg and around 5° S during the second leg. Therefore, the ITCZ shifted northwards by about 400 km, in a span of 12 days. A significant weakening in the ITCZ dynamics also occurred during the return leg of the cruise.

Significant spatio-temporal variability was observed in the mean fields and in the turbulent fluxes. We note that during both legs of the cruise, maximum fluxes were observed at the ITCZ. In both the legs there was a latitudinal gradient in the fluxes and they decreased gradually from the ITCZ towards 5° N. While the turbulent exchange coefficients, C_d and C_h, were found to be more or less constant with little scatter at wind speeds greater than 3 m s^{-1}, there was notable scatter in the values at lower wind speeds, as a result of the increased significance of their dependence on surface layer stability. This effect was most distinct near the Indian subcontinent on the return leg of the cruise, where the wind speeds were generally quite low (< 3 m s^{-1}). The *mean state* variables indicate that during each leg of the cruise, the dominant synoptic conditions were a result of northerly winds, blowing from the Indian subcontinent, interacting with the ITCZ in the southern hemisphere. In addition to this synoptic modulation, local features such as heterogeneity due to land masses and SST gradients lead to significant variability in the mean and turbulent fluxes.

The structure of the boundary layer was also found to vary depending on the various factors that influence the lower atmosphere. While the general trend was for the boundary-layer height to gradually increase towards the ITCZ, we note that other factors such as the warm pool of water (Equator to 5° S) and the proximity to land, influenced the boundary-layer structure. Over the warm pool we note a strong capping inversion on top of the boundary layer, while at the ITCZ the increased convection leads to a weaker capping inversion. The influence of continental air was also evident from the strong capping inversion and multiple mixed layers, observed north of 2° N. The presence of these continental air-masses in the form of plumes was noticed as far as 600 km offshore. These plumes were estimated to extend vertically from 1.5 km to 2.7 km. The diurnal variability in the boundary layer and the height of the trade inversion layer may control the lower and upper bounds and the thickness of such a plume. The advection of the anthropogenic aerosols and their interaction with the scattered marine stratus could prove to be an effective mechanism for entrainment and transport of aerosols into the deep convective clouds near the ITCZ. Away from land (south of 2° N), there was a good correlation between the thickness of the boundary layer and the surface sensible heat flux.

Diurnal variability was noted in most parameters in the lower atmosphere. Mean fields of temperature showed this trend in the surface layer throughout the cruise. The diurnal variability was also evident in the boundary-layer height, with a thicker boundary layer during daytime. The capping inversion was also found to vary diurnally with stronger inversion being observed during the early morning hours, thus indicating that the entrainment processes would be stronger in the afternoon than in the early morning. However, close to land the diurnal signal was not clearly evident. Land plumes appear to modulate the variation of the boundary layer by the formation of a strong elevated inversion.

Free convection was strongest at the ITCZ in both legs of the cruise. The strength of vertical mixing in the lower atmosphere is important since it helps determine the extent to which the measured surface concentrations of various aerosols are representative of the rest of the boundary layer. This is also true with the entrainment of fresh air at the top of the boundary layer. The entrainment velocities arrived at in this study, under clear atmospheric conditions, are at least an order of magnitude less than those observed on land. We know of no published estimates of entrainment velocities in this area, however these values are consistent with estimates from the Pacific Ocean (Huebert et al., 1996; Betts 1975) and Atlantic Ocean (Bretherton et al., 1995). Huebert et al. (1996) estimate entrainment velocities of about 0.005 m s^{-1} in the western Pacific and conclude that entrainment may be a major contributor (up to 80%) to the night-time reduced concentration of non-sea-salt aerosols in this area, dry deposition being the other factor. These estimates serve to emphasize that spatial variability in the boundary-layer height and the surface heat fluxes throughout the Indian Ocean, could play a critical role in initiating processes that may determine the vertical distribution of aerosols. Another effective form of entrainment of continental aerosols could be through the continental aerosol plume, which was noticed as far 600 km offshore. This thick air mass could interact with shallow convective clouds (over the Arabian Sea), which could ultimately feed into the deeper clouds at the ITCZ.

Significant spatial variability in most of the meteorological parameters throughout the cruise indicates dynamic land-ocean-atmosphere interaction. The magnitudes of the parameters depend primarily on the strength of the north-east monsoon and the ITCZ dynamics. The structure of the boundary layer was found to depend on local factors such as proximity to land and anomalous SST features, and on synoptic modulation by the ITCZ. We identify three regimes over the ocean where the boundary layer has distinct characteristics. As far as 600 km offshore it is modified by dry continental air masses; beyond this region the boundary layer is directly influenced by the presence of an anomalous warm pool (Equator to 5° S), and thirdly the ITCZ, where free convection leads to the thickest boundary layer.

Acknowledgements

The project was carried out under grants from ONR and the Atmospheric Science Division, NSF under grant ATM 962390. We would like to acknowledge the invaluable efforts by the crew of ORV Sagar Kanya. We would also like to thank the two anonymous reviewers for their insightful comments and suggestions, which have significantly improved this manuscript.

References

Betts, A. K.: 1975, 'Parametric Interpretation of Trade-Wind Cumulus Budget Studies', *J. Atmos. Sci.* **32**, 1934–1945.

Bradley, E. F., Coppin, P. A., and Godfrey, J. S.: 1991, 'Measurements of Sensible and Latent Heat Fluxes in the Western Equatorial Pacific Ocean', *J. Geophys. Res.* **96**, 3375–3389.

Bretherton, C. S., Austin, P., and Siems, S. T.: 1995, 'Cloudiness and Marine Boundary Layer Dynamics in the STEX Langrangian Experiments. Part II. Cloudiness, Drizzle, Surface Fluxes, and Entrainment', *J. Atmos. Sci.* **52**, 2724–2736.

Deadroff, J. W.: 1979, 'Prediction of Convective Mixed Layer Entrainment for Realistic Capping Inversion Structure', *J. Atmos. Sci.* **36**, 424–436.

Desjardins, R. L., MacPherson, J. I, Schuepp, P. H., and Karanji, F.: 1989, 'An Evaluation of Aircraft Flux Measurements of CO_2, Water Vapor, and Sensible Heat', *Boundary-Layer Meteorol.* **47**, 55–69.

Geernaert, G. L.: 1987, 'On the Importance of the Drag Coefficient in Air–Sea Interactions', *Dyn. Atmos. Oceans* **11**, 19–38.

Huebert, B. J., Wylie, D. J., Zhuang, L., and Heath, J. A.: 1996, 'Production and Loss of Mathanesulfonate and Non-Sea Salt Sulfate in the Equatorial Pacific Marine Boundary Layer', *Geophys. Res. Letters* **23**, 737–740.

IPCC, Climate Change: 1994, *Radiative Forcing of Climate Change and Evaluation of the IPCC IS92 Emmission Scenario*, John T. Houghton (ed.), 1995, Cambridge University Press, U.K., 399 pp.

Kang, I.-S., Kim, K.-M., and Kim, M.-K.: 1992, 'Estimation of Bulk Exchange Coefficients in the Western and Eastern Tropical Pacific Using ATLAS Buoy Observations', *TOGA Notes* **9**, 1–3.

Krishnamurti, T. N., Jha, B., Prospero, J. M., Jayaraman, A., and Ramanathan, V.: 1998, 'Aerosol and Pollutant Transport over the Tropical Indian Ocean during the 1996 Northeast Monsoon and the Impact on Radiative Forcing', *Tellus* **50**, 521–542.

Large, W. G. and Pond, S.: 1982, 'Sensible and Latent Heat Flux Measurements over the Ocean', *J. Phys. Oceanogr.* **12**, 464–482.

Liu, W. T., Katsaros K. B., and Businger, J. A.: 1979, 'Bulk Parametrization of Air–Sea Exchanges of Heat and Water Vapor Including the Molecular Constraints at the Interface', *J. Atmos. Sci.* **36**, 1722–1735.

Mohanty, U., Niyogi, D., Raman, S., and Sarkar, A.: 2000, 'Numerical Simulation of Land–Air–Sea Interactions over the Indian Ocean during the North-Easterly Monsoon during INDOEX', *Curr. Sci.*, in press.

Panofsky, H. A., Blackadar, A. K., and McVehil, G. E.: 1960, 'The Diabatic Wind Profile', *Quart. J. Roy. Meteorol. Soc.* **86**, 390–398.

Paulson, C. A.: 1970, 'The Mathematical Representation of Wind Speed and Temperature Profiles in the Unstable Atmospheric Surface Layer', *J. Appl. Meteorol.* **9**, 858–861.

Ramanathan, V., Crutzen, P. J., Coakley, J., Dickerson, R., Heymsfield, A., Kiehl, J., Kley, D., Krishnamurti, T. N., Kuettner, J., Lelieveld, J., Mitra, A. P., Prospero, J., Sadourny, R., Valero, F. P. J., and Woodbridge, E. L.: 1995, 'Indian Ocean Experiment (INDOEX)', White Paper, July 1995.

Roswintiarti, O., Niyogi, D., Raman, S., and Mohanty, U.: 2000, 'Application of a Three Dimensional Triple Nested Mesoscale Model (MM5) for Assessing the Transport and the Boundary Layer Variability over the Indian Ocean during INDOEX', *Curr. Sci.* (INDOEX Issue), in press.

Smith, S. D.: 1988, 'Coefficients for Sea Surface Wind Stress, Heat Flux and Wind Profiles as a Function of Wind Speed and Temperature', *J. Geophys. Res.* **93**, 15467–15472.

Stull, R. B.: 1976, 'The Energetics of Entrainment across a Density Interface', *J. Atmos. Sci.* **33**, 1268–1278.

Stull, R. B.: 1988, *Introduction to Boundary Layer Meteorology*, Kluwer Academic Publishers, Dordrecht, 666 pp.

Zhang, G. J. and McPhaden, M. J.: 1995, 'The Relationship between Sea Surface Temperature and Latent Heat Flux in the Equatorial Pacific', *J. Climate* **8**, 589–604.